

Chapter 1. Global agroclimatic patterns

Chapter 1 describes the CropWatch Agroclimatic Indicators (CWAIs) rainfall (RAIN), temperature (TEMP), and radiation (RADPAR), along with the agronomic indicator for potential biomass (BIOMSS) in sixty-five global Monitoring and Reporting Units (MRU). Rainfall, temperature, and radiation indicators are compared to their average value for the same period over the last fifteen years (called the “average”), while BIOMSS is compared to the indicator’s average of the recent five years. Indicator values for all MRUs are included in Annex A table A.1. For more information about the MRUs and indicators, please see Annex C and online CropWatch resources at www.cropwatch.com.cn.

1.1 Overview

CropWatch Agroclimatic Indices (CWAIs) are averages of climatic variables over agricultural areas only (refer to Annex A for definitions and to table A.1 for 2018 July to October (JASO) numeric values by MRU). Although they are expressed in the same units as the corresponding climatological variables, they are spatial averages, weighted by the agricultural production potential. For instance, in the “Sahara to Afghan desert” area, only the Nile valley and other cropped areas are considered. “Sahara to Afghan desert” is one of the 65 CropWatch Mappings and Reporting Units (MRU), which are the largest monitoring units adopted to identify global climatic patterns. They have listed in annex A.

Correlations between variables (RAIN, TEMP, RADPAR) at MRU scale derive directly from climatology. For instance, the positive correlation ($R=0.391$) between rainfall and temperature results from high rainfall in equatorial, i.e. in warm areas. Therefore, this description of very large global climatic patterns focuses on departures from average variables, i.e. anomaly patterns which characterize the current reporting period more meaningfully than the averages themselves.

RAIN was below average in about 63% of the MRUs, nevertheless resulting in RAIN being 12% above the average value of the 15-year reference period (2003-2017) over agricultural areas¹ (Table 1.1). The high-value results from few very large departures in some semi-arid areas such Southern Mongolia (620 mm or +180% in MRU 47), Gansu-Xinjiang (367 mm or +121% in MRU 32) and the southern Mediterranean (185 mm or +88% in MRU 07). TEMP was slightly below average (-0.1°C) in most MRUs (63%) while RADPAR was above average in 66% of the MRUs resulting in 1% above average sunshine. This is the first positive sunshine departure in about two years. Because MRUs are large areas, and because sunshine tends to be less variable than rainfall or temperature, a 1% departure is more significant than it would be for rain. Finally, the biomass production potential BIOMSS depends on rainfall and temperature. During the current reporting period, 72% of its variations can be ascribed to RAIN variations and just 1% to TEMP. The global biomass accumulation potential is just 6% above normal, resulting from contrasting spatial patterns of the climatic variables (Table 1.1 and text below).

During the current JASO reporting period, rainfall anomalies tend to be negatively correlated with TEMP and with RADPAR departures, indicating the expected association between drought and high temperature and sunshine.

Table 1.1: Departure of RAIN, TEMP and RADPAR indicators from their recent 15-year averages over the last two years (average of 65 MRUs, unweighted)

| Reporting period | | CropWatch Indicator | | |
|------------------|------|---------------------|--------|--------|
| | year | RAIN | TEMP | RADPAR |
| JFMA | 2017 | 0.13 | -0.2°C | -0.02 |
| AMJJ | 2017 | 0.09 | -0.1°C | -0.02 |
| JASO | 2017 | 0.06 | +0.1°C | -0.03 |

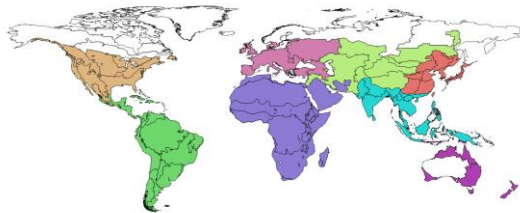
| | | | | |
|-------------|---------|------|--------|-------|
| ONFJ | 2017-18 | 0.08 | -0.1°C | -0.04 |
| JFMA | 2018 | 0.08 | -0.1°C | -0.05 |
| AMJJ | 2018 | 0.05 | -0.2°C | -0.03 |
| JASO | 2018 | 0.12 | -0.1°C | 0.01 |

Reporting period

Above average RAIN is the continuation of a pattern that started in 2017 (Table 1.1) but which undergoes significant spatial variations, as illustrated in Table 1.2. As mentioned above, some semi-arid areas benefit most from the increase through favorable rangeland development in areas where pastoralism prevails. However, other areas such as the West African Sahel (MRU 08, +17%), which are transition areas between pastoralism and crop agriculture benefit as well.

Table 1.2: Departures from the recent 15-year average of CropWatch agroclimatic indicators over regional MRU groups. Within each group, averages are weighted by the agricultural area of individual MRUs. “Others” include five non-agricultural areas shown in white in the map.

| | RAIN % | TEMP °C | RADPAR % | BIOMSS % |
|----------------------|-----------|-------------|-------------|-------------|
| Africa | 19 | -0.3 | 4 | 2 |
| America S + C | 10 | -0.5 | -1 | 19 |
| America N | 19 | -0.4 | -1 | 8 |
| Asia centre | 33 | -0.2 | -1 | 22 |
| Asia East | 2 | -0.2 | 2 | -7 |
| Asia South | -1 | -0.2 | -1 | -12 |
| Europe | -7 | 0.8 | 5 | 6 |
| Oceania | -34 | 0.2 | 3 | -11 |
| Others | 19 | 1.3 | 3 | 1 |
| World | 10 | -0.1 | 1 | 5 |



In addition to Boreal areas where crop agriculture is irrelevant (e.g. MRUs 57, 61 and 65, listed as “others” in table X.2), high temperatures occurred mostly in Europe. They were accompanied by high sunshine and water-stressed many crops on the continent. Regarding the biomass development potential, high values prevail in central Asia and Latin America while low values occur mostly in southern Asia and Oceania.

1.2 Main anomalies in individual MRUs

1.2.1. Precipitation deficits and excesses

In the MRUs listed below, BIOMSS anomalies roughly closely follow those of RAIN ($R=0.728$), take or give some percent. Few areas, however, that have atypical behaviors are specifically mentioned and also described in section 1.3 below.

The driest MRUs in relative terms (shortage in excess of 25%) occur on the west coast of North America (MRU 16), plagued by numerous ongoing forest and bushfires, Oceania (MRUs 54, Queensland to Victoria -35%; MRU 53, northern Australia -42% and MRU 56, New Zealand with a deficit reaching 68%) and Western Cape in South Africa. With the exception of MRU 16, all are characterized by low BIOMSS.

The southern hemisphere droughts are followed, in terms of severity, by the Caribbean (MRU 20, 24%) and three areas with deficits in the range of 10 to 16%. They occur in eastern Asia (MRU 43, East Asia and MRU 34, Huanghuaihai, China), the East African Highlands (MRU 02) and Europe, especially non-Mediterranean western Europe (MRU 60) and the Caucasus (MRU 29).

High rainfall occurred in Madagascar (MRU 05) and the semi-arid and arid areas from West Africa (MRUs 08 and 64, Sahel and Sahara to Afghan deserts), across the Middle-East and Central Asia (Pamir, MRU 30, and Gansu-Xinjiang, MRU 32) to eastern-central Asia (MRU 52). This continent-wide feature, which was highlighted in a number of previous CropWatch bulletins, seems to have become permanent.

In America Central-eastern Brazil (MRU 23, +31%) needs to be mentioned next to the northern Great Plains (MRU 12, +33%)

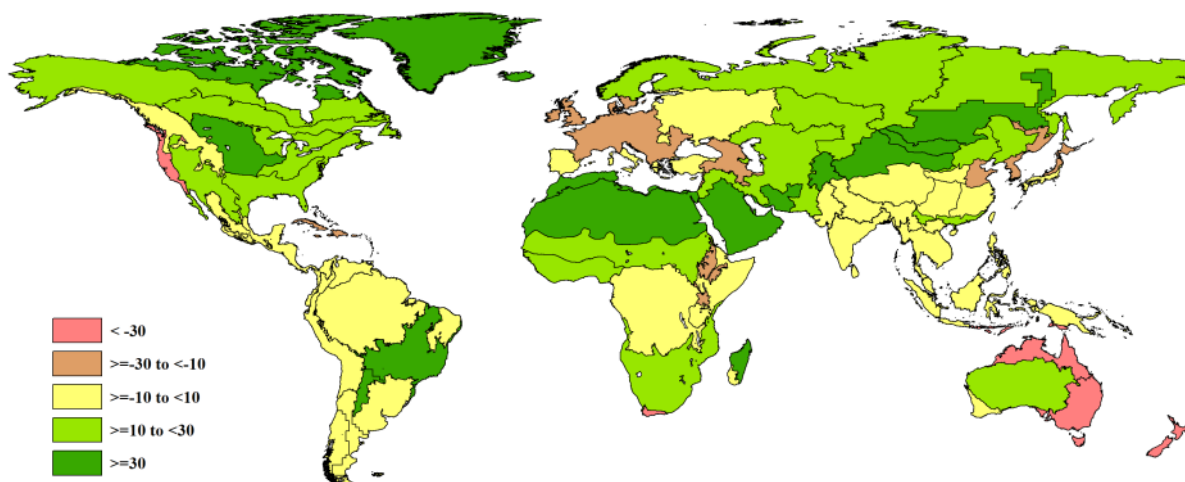


Figure 1.1: Global map of July-October 2018 rainfall anomaly (as indicated by the RAIN indicator) by MRU, departure from 15YA (percentage)

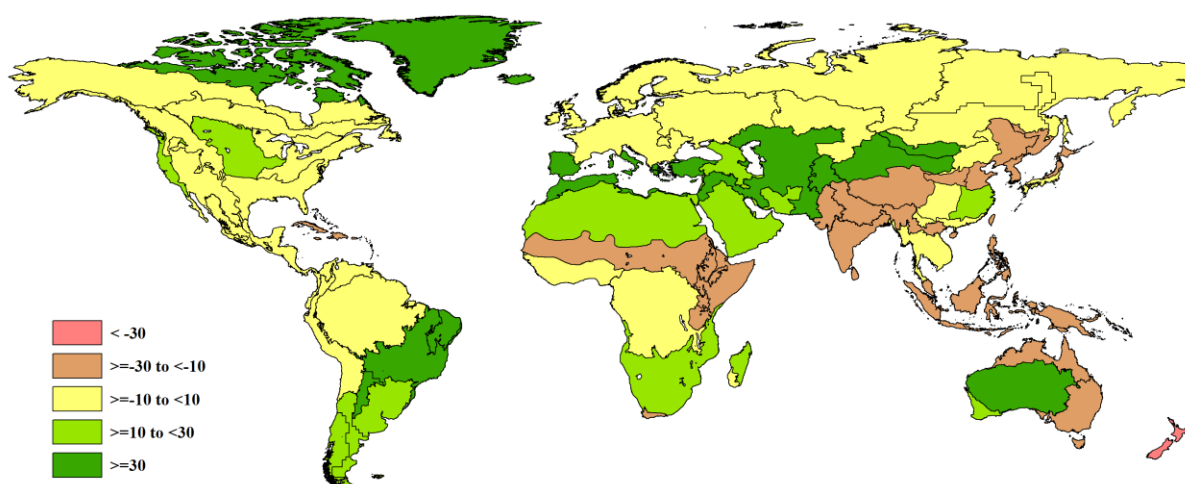


Figure 1.2: Global map July-October 2018 biomass accumulation (BIOMSS) by MRU, departure from 5YA, (percentage)

1.2.2 Temperature

As mentioned in the introduction, few extreme temperature departures need to be mentioned, if not for the rather rainy northern Great Plains (MRU 12, 1.2°C below average) and central northern Argentina (MRU 25), most of which is, however, not very relevant for crop production. Adjacent areas experienced relatively cool weather covering most of South America, but the drop is not sufficient to raise concern. The same applies to MRUs 03 (the Gulf of Guinea, -0.6°C), 04 (the Horn of Africa, -0.8°C) and 08 (the Sahel, -0.6°C).

In addition to two Mediterranean climate areas (Western Cape in South Africa, MRU 10, +1.2°C and Mediterranean Europe and Turkey, MRU 59, +1.3°C), Southern Japan and the southern fringe of the Korean peninsula (MRU 46) appear as a third area with a positive temperature departure worth mentioning at +1.8°C. Other areas with positive departures are located at high latitudes that are of no relevance for agriculture.

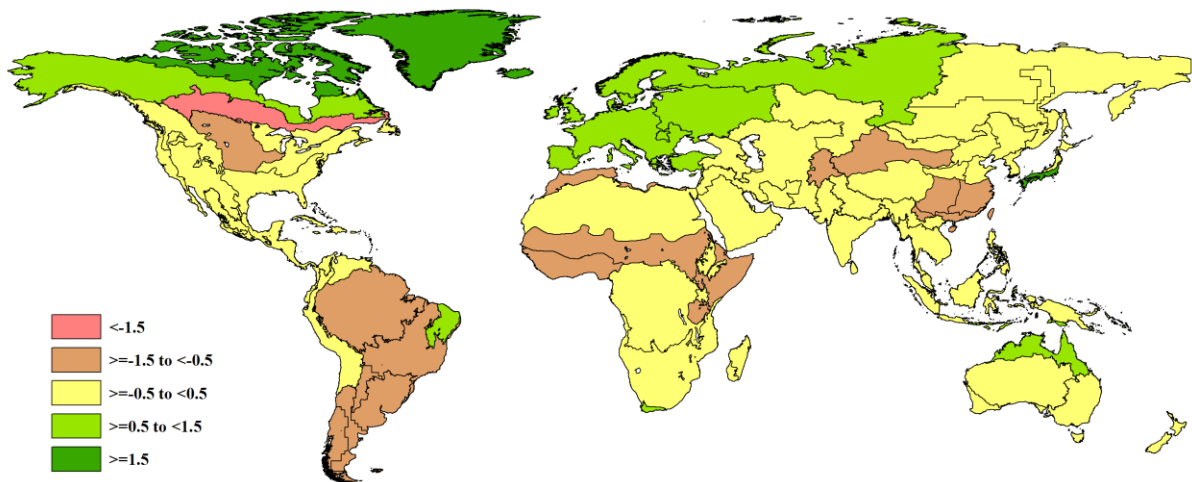


Figure 1.3: Global map of July-October 2018 air temperature anomaly (as indicated by the TEMP indicator) by MRU, departure from 15YA (degrees Celsius)

1.2.3 RADPAR

Relatively poor sunshine conditions are reported for some of the “cool wave” areas in Latin America, including especially MRU 25, central-north Argentina, with a very significant 9 % drop, as well as the Pampas (MRU 26) where the deficit reaches 6%.

Low RADPAR also occurred in MRU 48 (Punjab to Gujarat, -6%), as well as in the adjacent areas of the southern Himalayas (MRU 44, -3%), Southern Asia (MRU 45, -4%), MRU 39 (Qinghai-Tibet, -6%), MRU 40 (Southern China, -5%) and MRU 52 (Eastern Central Asia, -5%).

Deficits not exceeding 2% affected the central-eastern USA and Canada as well as northern Africa.

Large contiguous MRUs with above-average sunshine in the range from 4% to 8% occurred in essentially three areas: (1) the eastern fringes of Asia, south-east Asia, and Oceania, (2) northern-central Africa and Madagascar and (3) western Europe, extending east beyond the Ural Mountains. The largest anomalies (all at +7%) are those of the Gulf of Guinea countries (MRU 03), Western Europe (MRU 60) and especially New Zealand (MRU 56, +8%). An isolated occurrence with a large positive anomaly (+7%) affected the Caribbean islands (MRU 20).

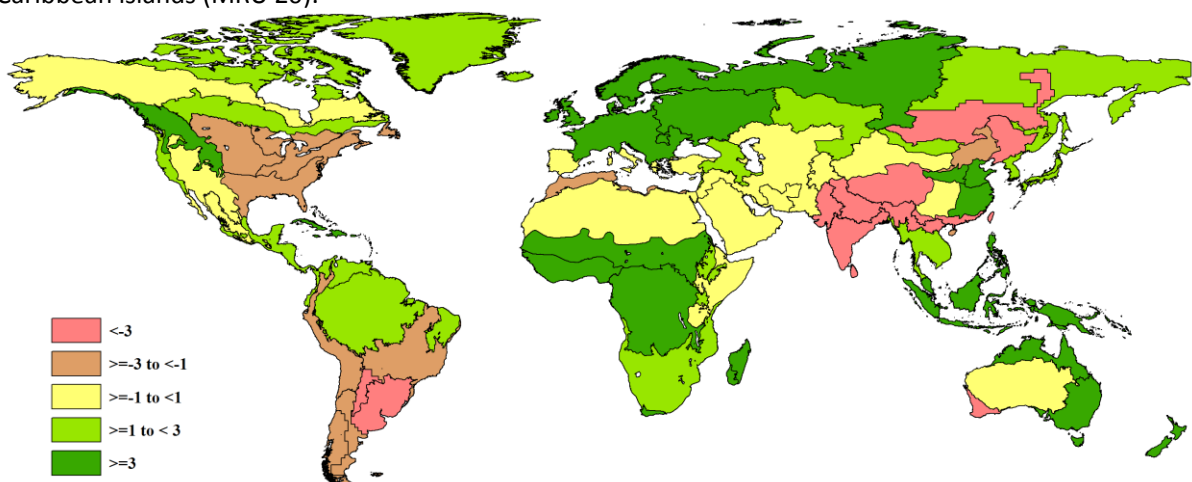


Figure 1.4: Global map of July-October 2018 PAR anomaly (as indicated by the RADPAR indicator) by MRU, departure from 15YA (percentage)

1.3 Combinations of extremes

One of the ways to look at global patterns is to cluster the MRUs based on the departures from the reference CWAI values. This done in figure 1.5 below where the paired RAIN-BIOMSS variables and RADPAR carry most of the variability.

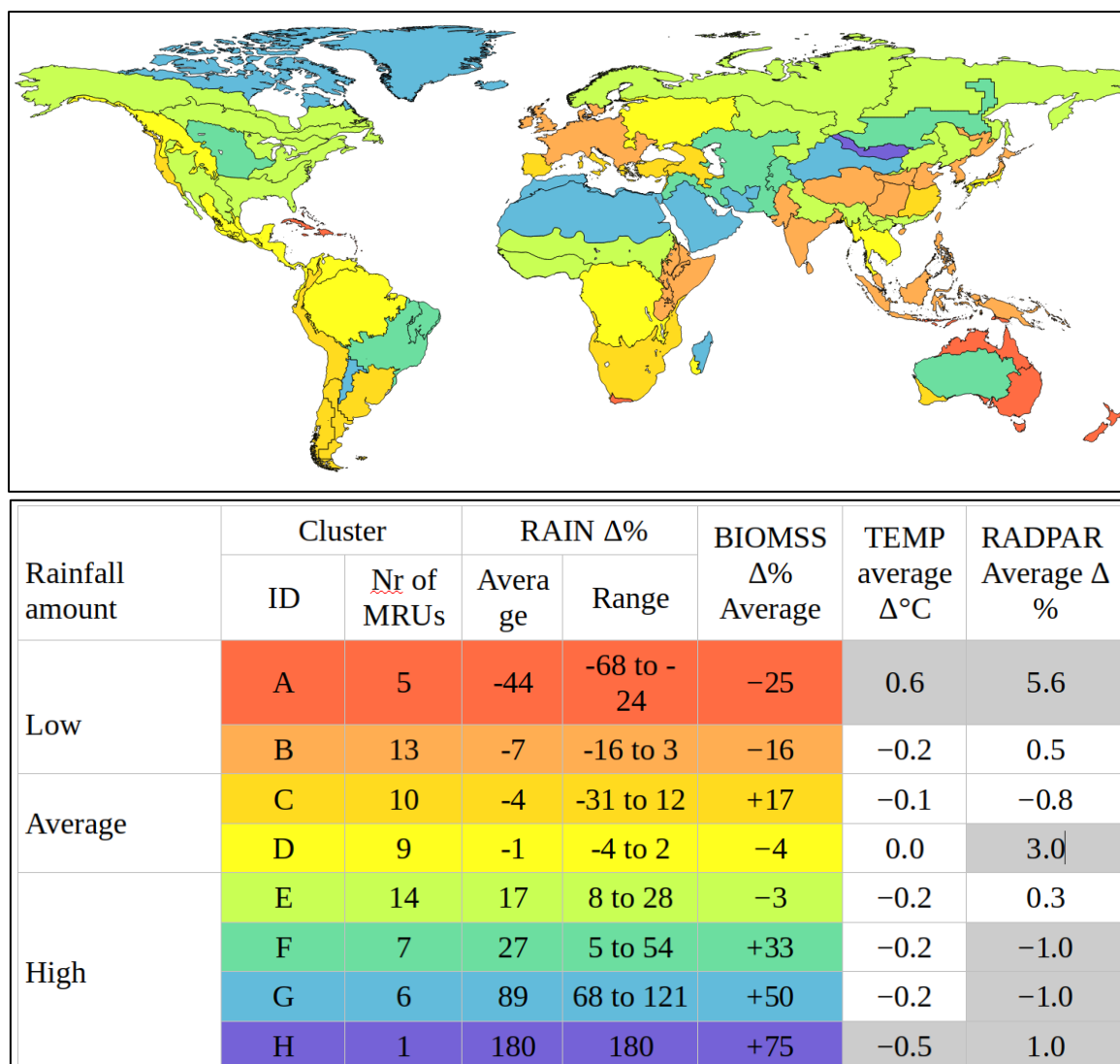


Figure 1.5: clustering of July-October 2018 CWAI anomalies in 65 MRUs into eight classes (standard hierarchical clustering using Ward's method based on Euclidean distances)

High rainfall areas (essentially the 13 MRUs in clusters F and G) are characterized by large BIOMSS departure values reaching 33% and 50% on average, which is significant. They cover mostly the already mentioned stretch from semi-arid and arid northern Africa to eastern central Asia in addition to patches in Latin America (MRUs 22, 23 and 25, the Brazilian Nordeste, central eastern Brazil and central north Argentina) and the northern Great Plains (MRU 12). On average, those locations experienced low sunshine and a slight reduction in temperature, with some exceptions such as the northern Great Plains where the temperature dropped 1.2°C below average and Central-north Argentina (MRU 25) where the deficit reached 1.4°C.

Considering its large rainfall excess (+68%) and the 9% drop in RADPAR, Central-north Argentina (MRU 25) is one of the most climatically abnormal spatial units for the current reporting period. More abnormal, actually than southern Mongolia, the one-MRU cluster H where only rainfall and biomass were exceptional.

Cluster E is the one with the largest number of MRUs (14). The slight positive rainfall anomaly combined with unfavorable temperature results in about average BIOMSS. The cluster includes some agriculturally unimportant areas at high latitudes. The most abnormal conditions for the cluster are those occurring in southern China (MRU 40) where both TEMP and RADPAR were unfavorable (-0.9°C and -5%, respectively) and in the Gulf of Guinea (MRU 03) where the RADPAR departure reached 7%.

Cluster D, includes essentially some tropical and equatorial MRUs (MRU 50, continental South-East Asia; MRU01, central Africa; and the three MRUs from the Amazon to Sierra Madre: 24, 19, 17) in addition to British Colombia to Colorado (MRU 11) and Ukraine to the Ural Mountains (MRU 58). The major abnormal conditions in this cluster are the +1.8°C temperature anomaly affecting MRU 46, Southern Japan and the southern fringe of the Korean peninsula, as well as the +6% sunshine departures in the two MRUs 01 (Equatorial central Africa) and 58, the area from Ukraine to the Ural mountains. Even with relatively high average RADPAR departure (+3%), cluster D is one of the most “average” of the current reporting period.

The MRUs in cluster C, are located at the “edges” of the continents in western North America, South America, southern Europe, and Southern Africa and eastern Asia. They are characterized by a good response of BIOMSS (+17%) to RAIN (+10%). The most abnormal conditions are those of the North American West Coast (MRU 16, RAIN -31%), temperature in southern Europe (MRU 59, +1.3°C) and low sunshine in two MRUs: -6% in the Pampas (MRU 26) and 5% in south-west Australia (MRU 55).

The most severe drought conditions are those associated with cluster A (RAIN down 44% on average), which covers a large area in eastern Oceania and two unconnected MRUs in Africa (MRU10, southern Cape area) and MRU 20 in the Caribbean. Almost all had high TEMP (especially MRU 10: +1.3°C) and abundant sunshine.

The MRUs in cluster B had consistently low rainfall, in spite of the moderate deficit of 7% on average, but variable RADPAR (-6% in MRUs 39 and 48, Qinghai-Tibet and Punjab to Gujarat, respectively; +6 and +7% in Huanghuaihai and western Europe, respectively). All MRUs underwent a drop in BIOMSS (-16%). The most abnormal conditions are those of Western Europe where rainfall was low and sunshine high, with a TEMP departure of 0.8°C.